Asymptotic normalization coefficients and neutron halo of the excited states in ^{12}B and ^{13}C

Z. H. Liu, C. J. Lin, H. Q. Zhang, Z. C. Li, J. S. Zhang, Y. W. Wu, F. Yang, M. Ruan, J. C. Liu, S. Y. Li, and Z. H. Peng
China Institute of Atomic Energy, P.O. Box 275(10), Beijing 102413, China
(Received 25 April 2001; published 21 August 2001)

The transfer reactions of ^{11}B$(d,p)^{12}$B and ^{12}C$(d,p)^{13}$C, at incident energy of 11.8 MeV, have been used to extract asymptotic normalization coefficients and root-mean-square radii for the last neutron in ^{12}B and ^{13}C. It is found experimentally that the second ($J^\pi=2^-$) and third ($J^\pi=1^-$) excited states in ^{12}B and the first ($J^\pi=1/2^+$) excited state in ^{13}C are the neutron halo states, whereas the third ($J^\pi=5/2^+$) excited state in ^{13}C is a neutron skin state.

DOI: 10.1103/PhysRevC.64.034312 PACS number(s): 21.10.Gv, 25.45.Hi, 27.20.+n

I. INTRODUCTION

The origin of the chemical elements in nature constitutes a fascinating problem of nuclear astrophysics. Among the various theories of element formation, stellar nucleosynthesis has become most successful and is now commonly accepted. In the theory, it assumes that only hydrogen, helium, and the rare light isotopes with $A<12$ are produced in the big bang; nuclei heavier than iron can only be created by successive neutron capture reactions and beta decay. The main reaction sequence to synthesis heavy elements ($A>12$) is

$$^1\mathrm{H}(n,\gamma)^2\mathrm{H}(n,\gamma)^3\mathrm{H}(d,n)^4\mathrm{He}(t,\gamma)^7\mathrm{Li}(n,\gamma)^8\mathrm{Li}(\alpha,n)^{11}\mathrm{B}(n,\gamma)^{12}\mathrm{B}(\beta^-)^{12}\mathrm{C}(n,\gamma)^{13}\mathrm{C},$$

etc. [1]. Along this sequence, the ^{11}B$(n,\gamma)^{12}$B and $^{12}C(n,\gamma)^{13}$C are two important reactions, especially the latter one [2,3].

So far, the capture cross sections of astrophysical interest for the ^{11}B$(n,\gamma)^{12}$B reaction are still unknown. For the ^{12}C$(n,\gamma)^{13}$C reaction, they have been measured by two groups [4–6] at neutron energies between 0.1 keV and 2 MeV. However, there are obvious discrepancies between these two sets of data [6]. Due to its importance as mentioned above, further experimental studies are strongly called for. However, the direct capture cross sections at stellar energies are very small, usually in μbarn. It is very difficult to measure them with high precission. Recently, Xu *et al.* [7] proposed an indirect method to obtain the direct capture cross section at stellar energy from the asymptotic normalization coefficient (ANC) of the overlap wave function in peripheral transfer reaction. The cross sections of the peripheral nucleon transfer at energies above the Coulomb barrier are several orders of magmitude larger than that of direct capture. Hence their method should provide an easy and reliable way to determine the capture cross sections of astrophysical interest.

In this work, we have measured the angular distributions of the transfer reactions ^{11}B$(d,p)^{12}$B and ^{12}C$(d,p)^{13}$C, and extracted ANC's for $^{12}\mathrm{B}\leftrightarrow{}^{11}\mathrm{B}+n$ and $^{13}\mathrm{C}\leftrightarrow{}^{12}\mathrm{C}+n$ from the measured differential cross sections at forward angles. We have also calculated the root-mean-square (rms) radii of the ground and excited states in ^{12}B and ^{13}C with these ANC's. Our results show that the second ($J^\pi=2^-$) and third ($J^\pi=1^-$) excited states of ^{12}B and the first ($J^\pi=1/2^+$) and third ($J^\pi=5/2^+$) excited states of ^{13}C are, respectively, the neutron halo or halolike states. Because the neutron capture in the *s* process follows the valley of beta stability, it would be very interesting to extend the investigation of the halo structure, as well as its effect on neutron capture, to the nuclear region on and off the β stability line.

II. EXPERIMENTAL PROCEDURE

The experiment was carried out with a collimated deuteron beam from the HI-13 tandem accelerator at China Institute of Atomic Energy, Beijing. The bombarding energy was 11.8 MeV. The thickness of the ^{11}B (with ^{12}C backing of 30 μg/cm^2) and ^{12}C targets was 215 μg/cm^2. Outgoing protons were momentum analized using a Q3D magnetic spectrograph. Two typical excitation energy spectra of proton are shown in Fig. 1. During the measurements at most of angles, two SSD's placed at $\pm 24°$ were used for monitoring the beam current. In the angular range of $15°\leqslant\theta_{Lab}\leqslant 35°$, instead of two, one SSD at $+24°$ was used. Except the SSD's, in the measurements at some angles, a Faraday cup set at 0° in the scattering chamber was used for determing the beam current directly.

The differential cross sections of the transfer reactions ^{11}B$(d,p)^{12}$B and ^{12}C$(d,p)^{13}$C were measured in the angular range of $5°\leqslant\theta_{Lab}\leqslant 140°$ in 5° steps. In the case of the $d_{5/2+}$ state of ^{13}C, the cross sections were measured at angles down to 0°. The counts of the elastic scattering at 24° were used for relative normalization of the transfer cross sections. The beam current measured by the Faraday cup along with the target thickness were used for the absolute normalization. The measured angular distributions of the transfer reactions

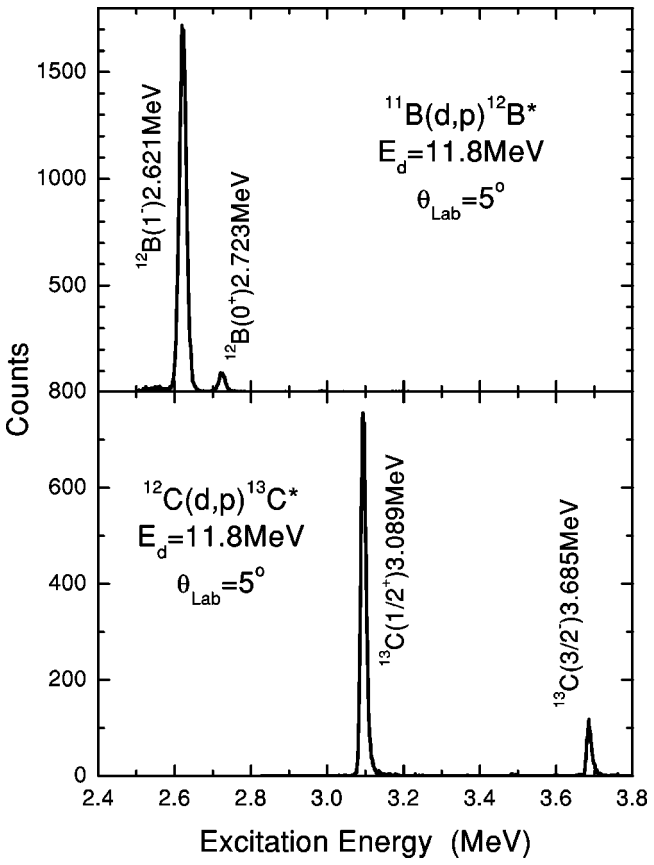

FIG. 1. The excitation energy spectra of proton from the ^{11}B$(d,p)^{12}$B and ^{12}C$(d,p)^{13}$C reactions measured by Q3D at 5°.

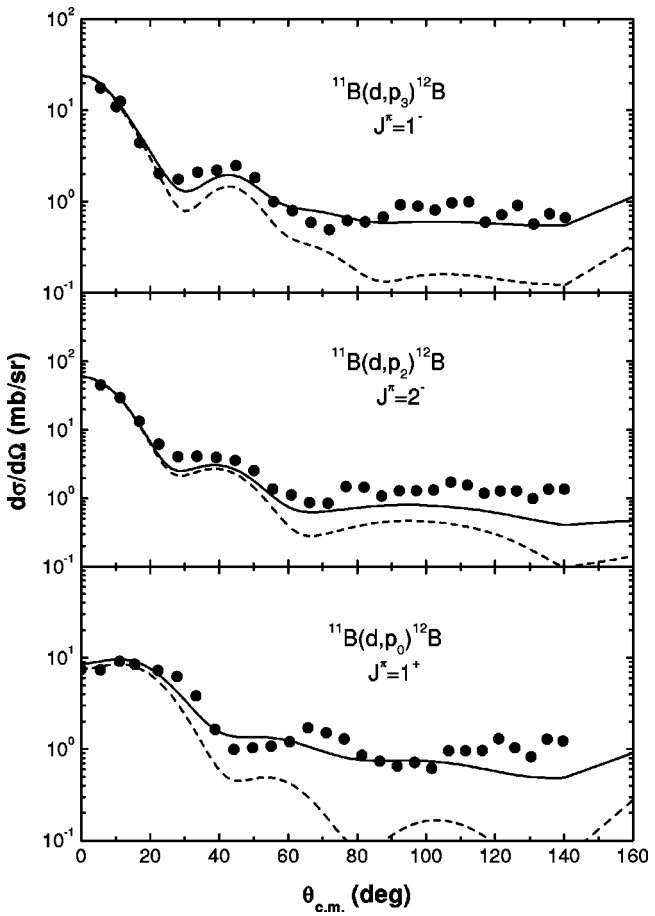

FIG. 2. Angular distributions for the transfer reactions ^{11}B$(d,p)^{12}$B at $E_d=11.8$ MeV. The dashed curves denote the normalized DWBA calculations, and the solid lines represent the results combining the contributions of the direct and the compound processes.

^{11}B$(d,p)^{12}$B and ^{12}C$(d,p)^{13}$C are, respectively, shown in Figs. 2 and 3 as solid points. The relative errors of the experimental data are about 6%, including the error of statistics, the uncertainties of the target thickness and the beam current measurement. Lang *et al.* [8] investigated the reaction ^{12}C$(d,p)^{13}$C at the deuteron energy of 12 MeV. Our results are in agreement with their data within experimental error.

III. EXTRACTION OF ANC'S

The experimental cross section for the peripheral transfer reaction $A(d,p)B$ can be expressed as

$$\frac{d\sigma_{exp}}{d\Omega}=(C^B_{Anl_Bj_B})^2(C^d_{pn})^2R_{l_Bj_B} \tag{1}$$

with

$$R_{l_Bj_B}=\frac{\sigma^{DW}}{b^2_{Anl_Bj_B}b^2_{pn}}, \tag{2}$$

where $C^B_{Anl_Bj_B}$, C^d_{pn} and $b_{Anl_Bj_B}$, b_{pn} are, respectively, the nuclear ANC's and the corresponding single-particle ANC's for $B\leftrightarrow A+n$ and $d\leftrightarrow p+n$ channels, l_B and j_B the orbital angular momentum and channel spin of the bound state $(A+n)$. As pointed out by Mukhamedzhanov *et al.* [9], $R_{l_Bj_B}$ in Eq. (1) is model independent for peripheral transfer reactions. $R_{l_Bj_B}$ can be calculated with a proper distorted-wave Born approximation (DWBA) code. Thus one can deduce $C^B_{Anl_Bj_B}$ as long as the transfer cross sections $d\sigma_{exp}/d\Omega$ are measured.

In the DWBA calculations, the exact finite range code PTOLEMY [10] is used. The optical model potential takes the form

$$U(r)=V_C(r)-Vf(x_v)+4iW\frac{d}{dx_i}f(x_i)$$
$$+\left(\frac{\hbar}{m_\pi c}\right)^2V_{s.o.}\frac{1}{r}\frac{d}{dr}f(x_{s.o.})\frac{\vec{l}\cdot\vec{s}}{s}, \tag{3}$$

where $f(x_j)=[1+\exp(x_j/a_j)]^{-1}$, $x_j=r-r_jA^{1/3}_{target}$, $j=v,i,s.o.$, and $V_C(r)$ is the Coulomb potential of a uniformly charged sphere with radius $r_{0c}A^{1/3}_{target}$. The potential parameters in the entrance channel were extracted from the elastic scattering data of $d+^{12}$C at an energy of 12 MeV [11]. The energy-dependent optical parameters of Goncharov *et al.* [12] are used to generate the distorted waves in the p

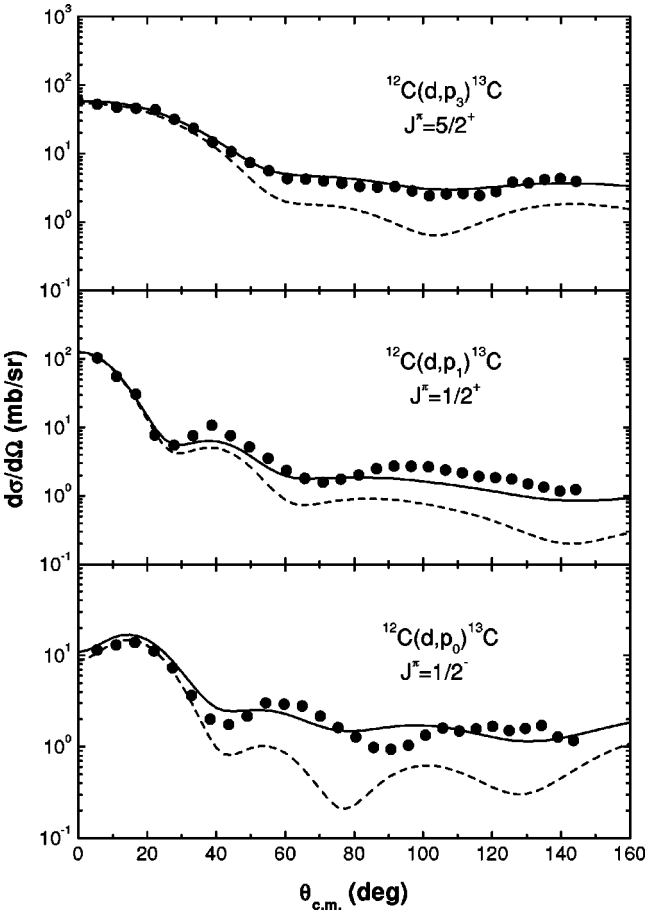

FIG. 3. Same as Fig. 2, but for the reactions ^{12}C$(d,p)^{13}$C.

$+^{12}$B and $p+^{13}$C exit channels. Listed in Table I are the values of the optical parameters used. The normalized results of the DWBA calculation are illustrated in Figs. 2 and 3 as dashed curves. In the same figures, the solid lines show the results combining the contributions of the direct and the compound processes. It is already known that the transfer differential cross section at forward angles is insensitive to the parameters of the distorted-wave optial potential [13]. It is just at these angles the value of ANC's is deduced. The single-particle wave functions are calculated with typical Woods-Saxon potentials. The depth of the potential is adjusted to reproduce the neutron binding energy. We vary the radius parameter r_0 and the diffuseness a of the potential on a grid of 12 points for $r_0=1.0$–1.3 fm and $a=0.5$–0.7 fm with 0.1-fm steps, respectively. In addition, the standard parameters of $r_0=1.25$ fm and $a=0.65$ fm are also used in our DWBA calculations. For each point on the grid, the single-particle wave function $\Phi_{n_Bl_Bj_B}(r,r_0,a)$ is obtained. Here the dependence of the $\Phi_{n_Bl_Bj_B}$ on the radius parameter r_0 and diffuseness a is explicitly indicated. The single-particle ANC $b_{l_Bj_B}$ can be deduced at large distance by its definition:

$$b_{l_Bj_B}(r_0,a)=\frac{\Phi_{n_Bl_Bj_B}(r,r_0,a)}{W_{-\eta_B,l_B+1/2}(2kr)/r},\quad r>R_N; \qquad (4)$$

here $W_{-\eta_B,l_B+1/2}$ is the Whittaker function, $k=\sqrt{2\mu\varepsilon_B}$ is the wave number, and μ, ε_B, R_N are, respectively, the reduced mass, binding energy, and the nuclear interaction radius for the bound state $(A+n)$. The Coulomb parameter η_B equals zero in the neutron case. The DWBA cross section σ^{DW} and single-particle ANC $b_{l_Bj_B}$ depend on the parameters of the binding potential, while their ratio $R_{l_Bj_B}$ does not.

As long as $R_{l_Bj_B}$ is obtained in the DWBA calculation, the nuclear ANC $C^B_{Anl_Bj_B}$ can be deduced from the experimental cross section with Eq. (1). We deduce the value of the ANC's from the differential cross sections at three forward angles ($\theta_{Lab}=5°$, 10°, and 15°). The value of $(C^d_{pn})^2$ for $d\leftrightarrow p+n$ is 0.76 fm^{-1} [14]. So the nuclear ANC $C^B_{Anl_Bj_B}$ for ^{12}B$\leftrightarrow^{11}$B$+n$ and ^{13}C$\leftrightarrow^{12}$C$+n$ is uniquely determined. The nuclear ANC's are model independent. Figure 4 shows the $b_{l_Bj_B}$, $S^{(sp)}_{l_Bj_B}$, and $C^B_{Anl_Bj_B}$ as a function of (r_0/a) for the third $(J^\pi=1^-)$ excited state of ^{12}B. The error bars are only due to the errors of measured cross sections. The obtained data of the $C^B_{Anl_Bj_B}$ are presented in Table II for various bound states of nuclei ^{12}B and ^{13}C. The errors listed in the table also include systematic uncertainties.

IV. NEUTRON HALO IN EXCITED STATES

A neutron or proton halo is bassically a threshold effect [15] resulting from the presence of a bound state close to the continuum. Therefore, except the nuclei near or at both the neutron and proton drip lines, a halo may appear in the excited state of stable nuclei, especially in $1/2^+$ state of light nuclei [16]. As mentioned above, to search for the halo structure of excited states in nuclei on and off the β stability line is of particular significance in astrophysics, as well as in nuclear physics itself.

In the single-particle approach [9], the nuclear radial overlap integral for $B\leftrightarrow A+n$ is approximated by a single-particle overlap integral,

$$I^B_{Anl_Bj_B}(r)\approx I^{B(sp)}_{Anl_Bj_B}(r)=[S^{(sp)}_{l_Bj_B}]^{1/2}\Phi_{n_Bl_Bj_B}(r). \qquad (5)$$

TABLE I. Optical model potential parameters.

Particle	V (MeV)	r_v (fm)	a_v (fm)	V_i (MeV)	r_i (fm)	a_i (fm)	$V_{s.o.}$ (MeV)	$r_{s.o.}$ (fm)	$a_{s.o.}$ (fm)
d	118.0	0.97	0.93	9.44	1.83	0.47	7.42	0.90	0.18
p	$66.535-0.108E_p$	1.006	0.654	$4.526+0.006E_p$	1.321	0.702	10.13	0.713	0.563

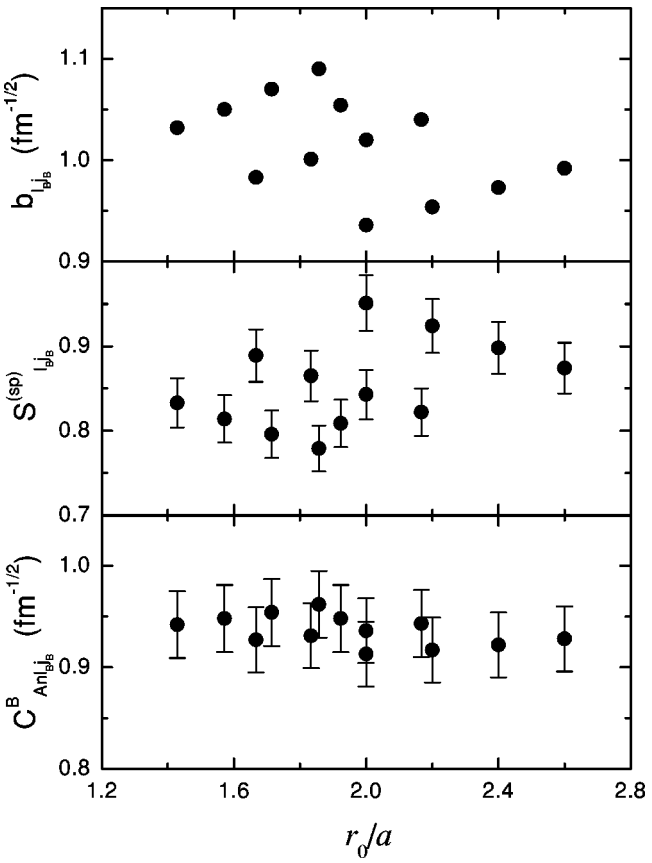

FIG. 4. The single-particle ANC ($b_{l_Bj_B}$), the single-particle spectroscopic factor ($S^{(sp)}_{l_Bj_B}$), and the nuclear ANC ($C^B_{Anl_Bj_B}$) as a function of r_0/a for the third excited state of ^{12}B.

The single-particle spectroscopic factor $S^{(sp)}_{l_Bj_B}$ relates the nuclear ANC and the single-particle ANC by

$$S^{(sp)}_{l_Bj_B}=\frac{(C^B_{Anl_Bj_B})^2}{(b_{l_Bj_B})^2}. \tag{6}$$

The rms radius of the last neutron in the orbital $(n_Bl_Bj_B)$ is defined approximately by the single-particle wave function,

$$\langle r^2\rangle^{1/2}\approx\left(\int_0^\infty r^4\Phi^2_{n_Bl_Bj_B}(r)dr\right)^{1/2}. \tag{7}$$

It can be separated into the contributions of the interior and the asymptotic region,

$$\langle r^2\rangle^{1/2}=\left(\int_0^{R_N} r^4\Phi^2_{n_Bl_Bj_B}(r)dr+(C^B_{Anl_Bj_B})^2\times\int_{R_N}^\infty r^2W^2_{-\eta_B,l_B+1/2}(2kr)dr\right)^{1/2}. \tag{8}$$

The first term in the equation is somehow parameter dependent. The parameters of the bound state potential adopted are not experimentally determined and can be varied. We calculate the first term by taking the set (r_0,a) so that $C^B_{Anl_Bj_B}=b_{l_Bj_B}(S_{l_Bj_B}=1)$. The second term is model independent, and gives major contribution to the rms radius. Thus the error introduced by the parameters used is small. The contribution of the asymptotic part of the wave function can be estimated by

$$D_\lambda(R_N)=\left(\frac{\int_{R_N}^\infty r^{2\lambda}\Phi^2_{n_Bl_Bj_B}(r)dr}{\int_0^\infty r^{2\lambda}\Phi^2_{n_Bl_Bj_B}(r)dr}\right)^{1/\lambda} \tag{9}$$

with $\lambda=1,2$. The D_1 represents the probability of the last neutron outside the range of the interaction radius R_N, and D_2 gives the contribution of the asymptotic part to the rms radius. Listed in Table II are the rms radii, the values of D_1, D_2 for the last neutron of the ground and excited states in ^{12}B and ^{13}C. It is worth noting that for the excited states with the orbital angular momentum $l_n=0$, D_1 is equivalent to or larger than 50%. In this sense [15] these states, i.e., the second ($J^\pi=2^-$) and third ($J^\pi=1^-$) excited states in ^{12}B and the first ($J^\pi=1/2^+$) excited state in ^{13}C should be the neutron halo states, while the third ($J^\pi=5/2^+$) excited state in ^{13}C is a neutron skin state. Dufour and Descouvemont [17] used the generator coordinate method to study ^{12}C$(n,\gamma)^{13}$C and obtain the mean distance between the ^{12}C core and the last neutron, $d=4.48$ fm for the $1/2^+$ excited state. Our result agrees with their value within the error.

TABLE II. Asmptotic normalization coefficients $C^B_{Anl_Bj_B}$, rms radii, D_1, and D_2 for the ground and excited states in ^{12}B and ^{13}C.

Nucleus	E_x (MeV)	l_n ($\hbar$)	J^π	$C^B_{Anl_Bj_B}$ (fm$^{-1/2}$)	$\langle r^2\rangle^{1/2}$ (fm)	D_1 (%)	D_2 (%)
^{12}B	0	1	1^+	1.16±0.10	3.16±0.32	19.9	70.2
	1.674	0	2^-	1.34±0.12	4.01±0.61	53.6	91.9
	2.621	0	1^-	0.94±0.08	5.64±0.90	66.8	96.3
^{13}C	0	1	$1/2^-$	1.93±0.17	3.39±0.31	14.3	62.1
	3.089	0	$1/2^+$	1.84±0.16	5.04±0.75	50.3	90.5
	3.854	2	$5/2^+$	0.15±0.01	3.68±0.40	25.2	74.2

V. CONCLUSION

We have measured the angular distributions of the peripheral transfer reactions ^{11}B$(d,p)^{12}$B and ^{12}C$(d,p)^{13}$C at 11.8 MeV, and derived the nuclear ANC's $C^{B}_{Anl_Bj_B}$ of the ground and excited states in ^{12}B and ^{13}C from the transfer cross sections at very forward angles. Our calculations show that the ANC value is insensitive to the parameters of the binding potential used. With these ANC's, we have calculated the rms radii, the probability D_1 of the last neutron outside the range of nuclear interaction, and the contribution, D_2 of the asymptotic part to the rms radius. Our results indicate that the second ($J^\pi=2^-$) and third ($J^\pi=1^-$) excited states in ^{12}B and the first ($J^\pi=1/2^+$) excited state in ^{13}C are the neutron halo states, whereas the third ($J^\pi=5/2^+$) excited state in ^{13}C is a neutron skin state.

The ANC method provides a natural way to relate the peripheral transfer reactions to the direct radiative capture reactions. It is of astrophysical interest to deduce the direct neutron radiative capture cross sections of ^{11}B and ^{12}C from the measured ANC's. The corresponding calculations are in progress.

ACKNOWLEDGMENTS

This work was supported by the National Natural Sciences Foundation of China (Grant Nos. 19875078 and 10075077) and the Major State Basic Research Development Program (Grant No. G200077400).

[1] R.A. Malaney and W.A. Fowler, Astrophys. J. **133**, 14 (1988).
[2] J.H. Applegate and C.J. Hogan, Phys. Rev. D **31**, 3037 (1985).
[3] T. Kajino, G.J. Mathews, and G.M. Fuller, Astrophys. J. **364**, 7 (1990).
[4] R.L. Mackin, Astrophys. J. **357**, 649 (1990).
[5] Y. Nagai, M. Igashira, K. Takeda, N. Mukai, S. Motoyama, F. Uesawa, H. Kitazawa, and T. Fukuda, Astrophys. J. **372**, 683 (1991).
[6] T. Ohsaki, Y. Nagai, M. Igashira, T. Shima, K. Takeda, S. Seino, and T. Irie, Astrophys. J. **422**, 912 (1994).
[7] H.M. Xu, C.A. Gagliardi, R.E. Tribble, A.M. Mukhamedzhanov, and N.K. Timofeyuk, Phys. Rev. Lett. **73**, 2027 (1994).
[8] J. Lang, J. Liechti, R. Muller, P.A. Schmelzbach, J. Smyrski, M. Godlewski, L. Jarczyk, A. Stralkowski, and H. Witala, Nucl. Phys. **A477**, 77 (1988).
[9] A.M. Mukhamedzhanov, C.A. Gagliardi, and R.E. Tribble, Phys. Rev. C **63**, 024612 (2001).
[10] R.P. Goddard, L.D. Knutson, and J.A. Tostevin, Phys. Lett. **118B**, 241 (1982).
[11] J.A.R. Griffith, M. Irshad, O. Karban, S.W. Oh, and S. Roman, Nucl. Phys. **A167**, 87 (1971).
[12] S.A. Goncharov, I.R. Gulamov, E.A. Romanovsky, N.K. Timofeyuk, and K.V. Shitikova, J. Phys. G **15**, 1431 (1989).
[13] H.T. Fortune and C.M. Vincent, Phys. Rev. **185**, 1401 (1969).
[14] L.D. Blokhintsev, I. Borbely, and E.I. Dolinskii, Sov. J. Part. Nucl. **8**, 485 (1977).
[15] P.G. Hansen, A.S. Jensen, and B. Jonson, Annu. Rev. Nucl. Part. Sci. **45**, 591 (1995).
[16] T. Otsuka, M. Ishihara, N. Fukunishi, T. Nakamura, and M. Yokoyama, Phys. Rev. C **49**, R2289 (1994).
[17] M. Dufour and P. Descouvemont, Phys. Rev. C **56**, 1831 (1997).